Received: 28 October 2022 | Revised: 9 May 2023 | Accepted: 21 June 2023

CAAI Transactions on Intelligence Technology

DOI: 10.1049/cit2.12261

The Institution of Engineering and Technology WILEY

ORIGINAL RESEARCH

D^2PAM: Epileptic seizures prediction using adversarial deep dual patch attention mechanism

Arfat Ahmad Khan[1] | **Rakesh Kumar Madendran**[2] | **Usharani Thirunavukkarasu**[3] | **Muhammad Faheem**[4]

[1]Department of Computer Science, College of Computing, Khon Kaen University, Khon Kaen, Thailand

[2]Department of Computer Science and Engineering, Rajalakshmi Engineering College, Chennai, India

[3]Department of Biomedical Engineering, Saveetha School of Engineering, Saveetha Institute of Medical and Technical Sciences (Deemed to be University), Chennai, India

[4]School of Technology and Innovations, University of Vaasa, Vaasa, Finland

Correspondence

Muhammad Faheem, School of Technology and Innovations, University of Vaasa, Vaasa 65200, Finland.

Email: muhammad.faheem@uwasa.fi

Abstract

Epilepsy is considered as a serious brain disorder in which patients frequently experience seizures. The seizures are defined as the unexpected electrical changes in brain neural activity, which leads to unconsciousness. Existing researches made an intense effort for predicting the epileptic seizures using brain signal data. However, they faced difficulty in obtaining the patients' characteristics because the model's distribution turned to fake predictions, affecting the model's reliability. In addition, the existing prediction models have severe issues, such as overfitting and false positive rates. To overcome these existing issues, we propose a deep learning approach known as Deep dual-patch attention mechanism (D^2PAM) for classifying the pre-ictal signals of people with Epilepsy based on the brain signals. Deep neural network is integrated with D^2PAM, and it lowers the effect of differences between patients to predict ES. The multi-network design enhances the trained model's generalisability and stability efficiently. Also, the proposed model for processing the brain signal is designed to transform the signals into data blocks, which is appropriate for pre-ictal classification. The earlier warning of epilepsy with the proposed model obtains the auxiliary diagnosis. The data of real patients for the experiments provides the improved accuracy by D^2PAM approximation compared to the existing techniques. To be more distinctive, the authors have analysed the performance of their work with five patients, and the accuracy comes out to be 95%, 97%, 99%, 99%, and 99% respectively. Overall, the numerical results unveil that the proposed work outperforms the existing models.

KEYWORDS

artificial intelligence techniques, classification, learning (artificial intelligence)

1 | INTRODUCTION

A general neurological disorder is Epilepsy, and it poses considerable effects on the economy and society [1] along with having different underlying causes [2]. There is a neuronal activity which is based on abnormal and excessive as a result of Epileptic seizure in the brain cortex, and it can be confirmed using the EEG (scalp electroencephalogram) [3], EEG (stereo-electroencephalography) [4], or ECoG (electrocorticography) [5]. Interestingly, studies are increased to use of the brain's signal data for many years to predict the seizure by the scalp EEG or the detection in earlier stages [1, 6, 7]. A crucial requirement motivates the effort for giving the medical experts and patients the reliable warning when the time between the onset of disabling symptoms in patients for the intervention on time and starting the measured evolution of ictal in the brain signal to change the evolution of seizure potentially [6]. This study provides insights into understanding the mentioned techniques for the propagation and initiation of the seizure [1].

Early detection or the prediction of reliable seizures is difficult in a computational way, despite the increase in the enhancement of the algorithms and devices over the decades. Primarily, there is great susceptibility to different sources of bioelectric noise, difficulties of considerable posing in the brain activities interpretation and analysis [8] during the recordings of the scalp EEG that are used daily. There is a long-established EEG approach to obtaining electro-physiological signals from brain region, and the activities are recorded with less noise over scalp EEG. Moreover, the EEG signals vary from patient to patient, which can be large due to the implantation of the EEG electrodes depending on the zone of epileptogenic that differs between the patients. The broad distribution of demographic and different kinds of epilepsy patients raises the high variance from patient to patient. Secondly, the open question is the process of detecting the early seizure. Although the trained neurologist finds the spikes of pre-ictal having 60 min before the seizure onset, there are no existence of any proper definition for inter and pre-ictal periods [9]. The time window is determined based on the capability to perceive the brain signal changes and the seizure onset region. Thirdly, a restricted number of patients are having EEG and recorded seizures compared to the datasets of EEG, which is scaled that includes hundreds of patients in one research [2]. It is complicated to mobilise the previous analysis based on EEG for classifying the epileptic pre-ictal signal [10, 11].

The electrophysiological signals are captured directly by the approach of long-established called EEG through the implanted electrodes in a deep way using the surgery from the brain to the tissue of the brain [4]. The electrical activities are recorded, having considerable information and low noise over the scalp EEG. There are 15 years of seizure history obtained by the patient. The doctor put a few electrodes in the doubtful region to detect the lesion of Epilepsy. The electrode of EEG is inserted into the brain of humans, which has many contacts which are recorded that is 7–15 contacts having 3 mm centre-to-centre distance in a typical way with every shaft of the electrode such as A to J. The recordings of the EEG signal have greater amplitudes of 50–1500 μv and give alterations over the broad frequency range of up to 10 kHz [12].

Deep learning (DL) approaches have been highly successful in image classification tasks like medical imaging in recent years. Consider an example that the CNNs as convolutional neural networks are checked for having the great capacity for learning a higher level of features from the data of MRI and enhance the performance of the diagnosis of brain disease having the many author's efforts [13]. Moreover, the pre-defined ROIs are having the diagnosis of ES in a manual way by having the experience from experts for most of the previous methods of DL for implementing the diagnosis models based on CNNs that turn to inadequate significance of every difference with the help of similar space of template and that is not included the complete atrophy features related to the disease that is distributed in the complete brain. However, some methods of DL obtain the particular output for the locations of pathological that neglects the interpretability problems in the practices of medicine because of the characteristics of the black box for the neural networks. Furthermore, recent works on epileptic seizure prediction utilised enhanced DL algorithms which tend to overcome the class imbalance problems by extracting the geometric and handcrafted features [14, 15]. Widely, General Adversarial Networks and their enhanced versions were adopted; however, they are limited with stability issues [16, 17]. Some regions have structural changes in MRI scans that have great correlative features of pathological because brain atrophy happens locally in a general way. On the other hand, the remaining regions have less essential data for the distinction. Hence, the important difficulty for the diagnosis of MRI based on DL for improving the discriminative feature's identification has (i) informative microstructures having the regions locally, and (ii) essential regions in the image globally in a relative way.

1.1 | Research motivation

Accurate detection and prediction of brain seizures was a major concern in the state-of-the-art works. However, they inaugurate many researches works on brain seizure prediction using machine learning and DL algorithms, but they failed to attain the desirable accuracy. Some of the major research problems are listed in this section, which motivated us to propose a better research work. The research motivations are:

- High False Positive Rates: Almost many of the existing works extracts many features includes low level features, high level features etc., However, they were lacked with performing proper feature engineering (i.e. not analyse/discriminate the features properly), and it leads to discrepancies during prediction; therefore, causing higher false positive rates.
- Poor Classifiers: The existing works lack with adopting proper classifier for brain seizure detection/prediction. For instance, many of the existing works use conventional machine learning algorithms, such as Support Vector Machine (SVM), regression tress, KNN etc., However, the adoption of conventional machine learning algorithms leads to underfitting, interoperability, and they do not withstand with larger datasets causing class imbalance issues.

1.2 | Research contribution

D^2PAM(Deep dual-patch attention mechanism) is anticipated to mention the difficulties mentioned earlier in diagnosing ES by finding the pathological locations in a discriminative way. More particularly, there are three important components in D^2PAM: PAM as the attention module of multi-instance learning pooling, attention-aware global classifier, and PatchNets mentioned in Figure 1. D^2PAM can learn the structural features in a discriminative way from many patches of MRI locally that are distributed in the brain even though the PatchNets have the blocks of spatial attention. Thus, the features are provided with various weights to combine to the

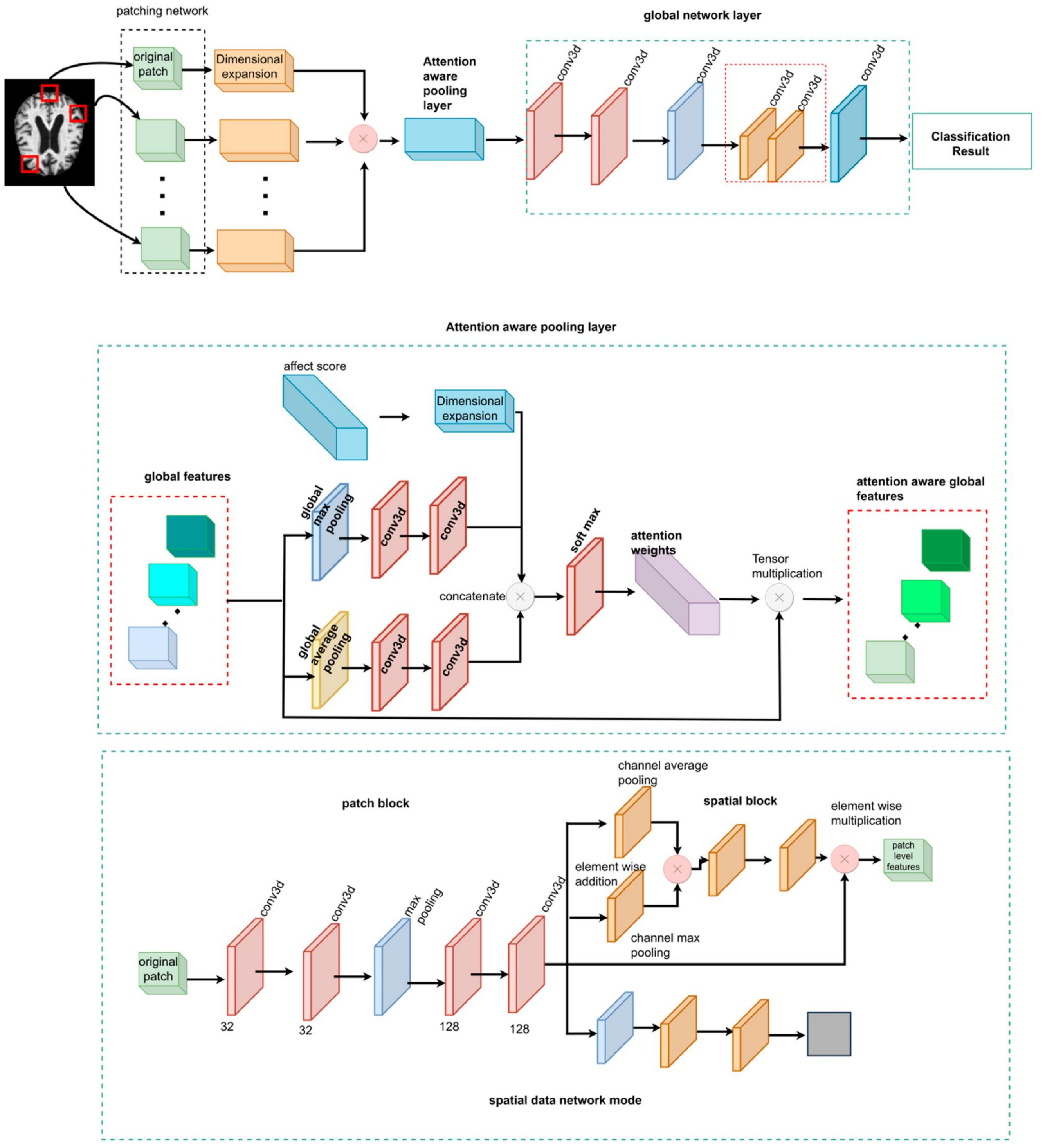

FIGURE 1 Architecture model

representation of global features via the pooling attention for the complete information related to brain structure depending on the global classifier to construct for the diagnosis of ES. The suggested technique is evaluated in the proposed method on two datasets from the public dataset, and the results from the experiments on many tasks of ES-oriented classification, such as prediction of MCI conversion and classification of ES, to implement the proposed methods of D^2PAM perform well than many modern methodologies in terms of generalisation and accuracy. Apart from the existing techniques, the proposed model gives the contributions that need to be summarised as below:

1) D^2PAM is the Deep dual-patch attention mechanism suggested to enhance the ES diagnosis performance that can automatically obtain the structural features from the scans

of sMRI globally and locally and maintain the decisions of classifications related to ES in the unified structure.
2) The designing of the Patch-Nets having blocks of spatial attention in every patch needs to extract the features in a discriminative way and improve the abnormal local features to change the micro-structures generated using brain atrophy.
3) *PAM* Operation such as patch attention mechanism is suggested for every patch with relative contribution to obtain the various representation of the weighted feature globally for the complete brain structure.

1.3 | Research organisation

The work is drafted as: Section 2 provides explanation of diverse approaches. In Section 3, the methodology is discussed with numerical results in Section 4. Section 5 belongs to the conclusions.

2 | RELATED WORKS

Some tools are modelled to characterise the seizure pattern from the brain signals. Moreover, many tools are concentrated on the data of scalp EEG. The characteristics of seizures are extracted by Oh et al. [13] from the newborn EEG using the representation of EEG signals with the help of Beta distribution in the domain of time and frequency. Singh et al. [18] designed a technique that depends on the decomposition of singular values used for dynamically searching the unique phases of humans' epileptic seizures. The similarities are identified in epileptic seizures. Spatio-temporal dynamics by Faust et al. [19] depends on EEG. The degree of time-varying non-linear correlation is evaluated by this method among the scalp electrodes, which is the onset and when spreading the seizure. A technique to detect the multivariate seizure is developed by Usman et al. [20] using the representation of the signals of EEG having the seizures of epileptic via the data of EEG analysis, and the methodology is the standard technique of machine learning to find the seizures from the data of EEG [21]. The use of simultaneous EEG scalp in patients is accessed by Duan et al. [22] having focal Epilepsy, which undergoes the evaluation of intracranial EEG after the presurgical testing in a detailed way. The transition to seizure from normal, identified by Zhang et al. [23], is not an immediate phenomenon. Apart from this, there is a procedure with resilience progressive loss of the neural network. A generalised retrospective based on CNN, and a model of seizure classification based on the patient is used by Usman et al. [24] with the help of data from scalp EEG and intracranial information.

There is no chosen method directly for analysing the data of EEG even though the previous tasks provided the seizure patterns of EEG in a detailed way due to (i) the fixed position of the EEG channel. On the other hand, the electrodes of EEG are implanted in the anato-electro-clinical research has a detailed analysis for the zone of epileptogenic potentially of each patient [25], (ii) the EEG has a sampling frequency which is lesser than EEG [26], (iii) When using the trained model for the new patients, the parameter has adjusted in a manual way that is unavoidable even now [27]. Some researchers are tried to find the patterns of seizure in the data of EEG. The collaborative application has a rich and dedicated interface of intuitive graphics that are provided for the analysis to record the brain with ECoG, EEG, and EEG called Brainstorm [28]. The MNE tool [29] is used to visualise, explore, and analyse the data on neurophysiology. A tool is used by Yildirim et al. [30] to predict the timing of seizures and find the areas of epileptic using the data of EEG. The classification tool of epileptic seizures is for analysing the spectrum of power from the signals of EEG as stated by Baratloo et al. [31]. Moreover, these tools have restricted applicability because of the high complexity of data [32]. These drawbacks need to be resolved using the proposed model (Tables 1 and 2).

3 | MODEL DESIGN

To handle the issues encountered in the existing approaches, this work proposes a novel D^2PAM to predict the appropriate features for ES prediction. The proposed model contains three diverse modules: patch network, pooling and attention module with global classifier. The patch level pattern analysis with attention blocks helps to learn the discrimination among the features from various patches. The patch-level features are provided with various weights and merged with the global feature representation from the entire structure based on the global classifier for ES prediction. The performance of the proposed model is compared with online available dataset and the outcomes are related to prediction process. The proposed model outperforms various existing approaches in terms of generalisation and performance. The proposed D^2PAM is used in the proposed system with complete architecture and important components, and the loss function depends on the learning of multi-instance and the mechanisms' attention. Lastly, the implementation details are provided in the proposed model.

The patch-level pattern analysis of brain morphometrics is done to diagnose ES in the proposed system as the multi-instance issue. The proposed methods are constructed depending on multi-instance learning. The set of bags are in training data as $D = \{(X_i, Y_i)\}_{i=1}^{N}$, the ith bag or sample is represented by X_i, and Yi represents the bag-level label of X_i. Every bag has many unlabelled instances, such as $X_i = \{I_{i,j}\}_{j=1}^{N}$; here, the jth instance is represented by $I_{i,Nipresentsj}$ and the number of instances in X_i. Rather than this, there are positive instances (at least one) and negative samples in the positive and negative bag. When $\sum_{j=0}^{N_i} Y_{i,j} = 0$, the $y_{i,j}$ is denoted in the proposed system. Here, the instance-level label of $I_{i,j}$ is represented by $y_{i,j}$. Else, $Y_i = 1$. A few local regions are occurred by abnormal brain atrophy, particularly in the earlier phases of ES. The bag of patches is concerned in the proposed system as the positive bag from the particular MR image of

TABLE 1 Summary of existing works in epilepsy.

References	Data	Algorithms	Dataset utilised	Limitations	Prediction accuracy
Freestone et al. [1]	EEG record	Regression tree, Bayesian network, Artificial neural networks, k-NN	ECoG dataset	• High false positive rates as the features were not engineered properly	85%
Kuhlmann et al. [2]		Support Vector Machine (SVM) and Local Binary patterns	-	• Poor characterisation of seizures features leads to poor classification	89%
Usman et al. [20]		SVM, Multi-layer perceptrons, and logistic model tree	CHB-MIT dataset	• Only limited features were extracted thereby chance of ineffectiveness in seizures detection	95%
Cui et al. [21]		SVM	Kaggle seizure prediction challenge dataset and CHB-MIT dataset	• Less stability as it lacks synchronisation	79%
Assi et al. [25]		Linear mixed model	-	• High heterogeneity issues	68%
Oh et al. [13]		Radial bias network and SVM	Real time data acquired from 3 to 37 children	• Not suitable for larger dataset samples	60%
Malasinghe et al. [10]		Ensemble classifier	-	• Higher computation complexity issues	80%
Acharya et al. [9]		Genetic algorithm and PSO with SVM	CHB-MIT dataset	• Less convergence • Underfitting issues	83%
Zhou et al. [3]		Deep learning	Bonn dataset	• Higher time consumption	88.5%
Freestone et al. [1]		Correlation dimension	-		90%
Gao et al. [6]		Recurrent neural networks	CHB-MIT	• Higher time consumption	92%
Proposed work	EEG record	Deep Dual Patch Attention Mechanism (a deep learning approach)	Bonn dataset	-	99%

TABLE 2 Algorithms used for comparing the performance parameters with the proposed deep dual-patch attention mechanism.

References	Technique utilised
[31]	Support Vector Machine (SVM)
[32]	CNN-based voting
[33]	Deep Convolutional Neural Network (DP-CNN)
[34]	Partial Interpretable Estimators (PIES)
[36]	Long Short-Term Memory (LSTM)
[35]	Individual Transformer
[33]	Diffusion Convolutional Neural Network (D-CNN)
[37]	ED-ANN with LSTM
[38]	ED-ANN with transformer

patients. Accordingly, the patches are grouped into the negative bag from the normal control in the proposed system. Then, many patches in bags have the labels of bag level that occurred as the large images like the trained data for the diagnosis based on ES.

The suggested model of D^2PAM that is presented in Figure 1 has four important stages that have instance selection to compose a bag X that is Patch Location Proposals, and the instance-level features have transformation f that is Patch-Net, the transformed instances have the combination φ that is described attention pooling, the combined bag level features are used for the classification g such as Attention-Aware Global Classifier presented. The positive classification has the probability Θ is presented as $\Theta(X) = g\varnothing f(X)$.

3.1 | Patch analysis

The initial selection of patches from the scans is used by Patch location proposals as the input for the proposed system. A theoretical methodology is proposed using the patch extraction to concern the set of comparisons on the patches rather than the features based on voxelwise. The image of MR is divided uniformly in the proposed system into many patches (fixed size)as $W \times W \times W$, with no intersection for simplifying the calculations and eliminating the relevant data. Moreover, the partitioned patches are not relevant to the atrophy, which is abnormal and is created by ES. A considerable difference between the control and experimental groups is found in the test method. The patch locations in the proposed experiment have a more considerable difference between the group of ES in the brain's abnormal atrophy regions. Then, the t-tests are used in the proposed system for sorting all the patches information. The voxel-wise features have the average to compute in the proposed system in one patch, like the feature related to the patch level. Comparing the two groups of features based on patch level is grouped in patch location accordingly to the patients with ES and general controls using the t-test in the training set. The $p-$ value is obtained in the proposed system at the patch location that presents the location information. The computation of all the $p-$ values is done on all the normalised locations using the $\frac{p_{\text{value}}-\text{MIN}}{\text{MAX}-\text{MIN}}$ and forming the map of $p-$ value to cover the complete brain image of MR. In addition, the small $p-$ values have the locations to consider roughly for greater discrimination. The number of patches is chosen in the proposed system based on the map of $p-$ value at the locations in one image having the small $p-$ values for composing the bag, such as $X = \{I_1, I_2, \cdots, I_k\}$ here, the number of chosen patches is presented by k and $I_i \in R^{W*W*W}$ in the proposed model as the input.

3.2 | Spatial patch network model

The Patch-Net structure, shown in Figure 1, has the spatial attention block. The Patch-Net has two tasks such as (i) learning the spatial attention-aware to represent the patch-level feature, and (ii) the effect score is the output to indicate the capability to trigger the label of the bag. The blocks of spatial attention are utilised to enhance the feature for the discriminative parts in the patches having a fixed size. The proposed D^2PAM methodology has all the Patch-Nets with similar architecture.

1) Patching Net: More abstract representations of features are learned using PatchNet, alike the former part as the backbone from original patches and lowering the feature map's size. It has four layers of 3D convolutional, and the patches have max pooling to choose the input patches size. The primary convolutional layer consists of the size of the kernel as 4 × 4 × 4. There are three layers of convolutional with a similar filter size as 3 × 3 × 3. The filter size is 2 × 2 × 2 during down sampling. The total channels (conv1 to 4)are 32, 64, 128 *and* 128 where the layers' training is done in the unit stride, having the feature maps of non-zero padding. ReLU (rectified linear unit) and Batch normalisation (BN)activations follow every convolutional layer. The two branching modules are extended by Patch-Net depending on the output of feature maps from conv4. This work presents one of the spatial blocks of attention to learn the patch-level representation of spatial attention-aware that is $C \times w \times w \times w$ as size here, the number of channels is presented as C, and the feature maps' size is presented as $w \times w \times w$. Another module has the global pooling, sigmoid function, and the fully connected layer (FCL) concentrated on generating the affect score that is utilised for finding the pathological locations in a discriminative manner. The Patch-Nets give the output from the local patch-level features to handle the three-dimensional shape to learn the spatial relationship between patches and also for the best combination of patches rather than creating one-dimensional feature vectors in many previous transforms based on instance level.
2) Spatial channel and maximal pooling: The spatial attention block is designed in the proposed system to embed into the proposed Patch-Net that is motivated by the proposed module of spatial attention for choosing the feature extraction related to local structure from the image patches of 3D. The block of spatial attention has the architecture presented in Figure 1. There are two various pooling with the axis of the channel that is average channel pooling and max channel pooling which are chosen for creating the two maps of feature in the average features and max features name accordingly. Thus, the concatenation of the two maps of features is done by having the $2 \times w \times w \times w$ size as the input for the consecutive convolutional layer that is padding: 1 to maintain the feature maps size and stride: 1, size of the kernel as 3 × 3 × 3. The convolutional layer has the output that is concerned like the map of spatial attention like the similar size as the maps of feature from conv4, ($A_{spatial} \in Rw \times w \times w$) having the score of attention at every location to be restricted to the range ($0 \rightarrow 1$) via the sigmoid layer. The spatial varying of various parts in the patch is described by the map of spatial attention that gives the feature representations which is multiplied element-wise in the conv4 output having the aspatial attention map computed to represent the local spatial attention-aware in a structural way created ultimately. Thus, the suggested block of spatial attention is explained in the proposed system having different formulae. The conv4 has the output denoted as $F = \{F_1, F_2, \cdots, F_C\}$, here, the number of channels is presented as C and $F_i \in R^{w*w*w}$. The expression of max pooling with the axis of the channel is presented below:

$$F_{\max} = \text{channelMaxpooling}\,(F) \tag{1}$$

Here, $F_{\max}^{w,h,l} = max\left\{F_1^{w,h,l}, F_2^{w,h,l}, \ldots, F_C^{w,h,l}\right\}$. The representation of the average pooling with the axis of the channel is given below:

$$F_{\text{average}} = \text{channelAveragePooling}\,(F) \tag{2}$$

Here, $F_{\text{average}}^{w,h,l} = \frac{1}{C}\sum_{c=1}^{C} F_c^{w,h,l}$. Thus, the two feature maps are concatenated in the proposed system and compute the map of spatial attention.

$$A_{\text{spatial}} = \sigma\left(W\left(\left[F_{\max}; F_{\text{average}}\right]\right)\right) \tag{3}$$

Here, the sigmoid activation is presented as σ, the convolutional layer weights W, and the concatenation is presented as [;]. The representation of the patch-level spatial-attention-aware feature F is given below:

$$F = \left[F_1 \otimes A_{\text{spatial}}; \ldots; F_C \otimes A_{\text{spatial}}\right] \tag{4}$$

Here, element-wise multiplication is represented as $\otimes$.

3.3 | Pooling

The patch-attention map is learned using the pooling operation and is proposed to represent that every patch has a relative contribution. Figure 1 shows the architecture of the pooling with attention. Every structural representation of patch level has the output as $F \in R^{C^*w^*w^*w}$ from Patch-Net to compress first using the average pooling with the axis of the channel to $\in R1 \times w \times w \times w$. Thus, the concatenation of the feature representation of the compressed patch level with the representation of global feature like Global $= \left\{\overline{F}_1, \overline{F}_2, \ldots, \overline{F}_C\right\}$, here, the number of patches are presented as C, and the ith input patch has the patch level features presented as $\overline{F}_i$. Since the empirical confirmation is there to exploit both the mentioned descriptors of feature to enhance the network's power representation over choosing one, that is, global maximum or global average are constructed parallel to create the two various descriptors of the feature. Thus, according to the two $1 \times 1 \times 1$ convolutional layers (CL), learns the two descriptors accordingly for producing the two maps of patch attention.

$$A_{\text{average}} = W_1 \text{ReLU}\left(W_0 GAP\left(F_{\text{global}}\right)\right) \tag{5}$$

$$A_{\text{max}} = W_1 ReLU\left(W_0 GAP\left(F_{\text{global}}\right)\right) \tag{6}$$

Here, W_0 and W_1 are used like the CL in the proposed system. Then, the CL share the parameters in feature descriptor processing with layers convolutional to process the descriptor of the max feature. The effectiveness score learned from every feature of intrapatch is concerned with evaluating the contribution of every patch rather than two maps of patch attention learned from the relationships of interpatch. All the Patch-Nets give the affect scores to create the effect vector as $a = \{a_1, \ldots, a_C\}$; here, total patches is C. The vector extension is done as a similar size to the maps of patch attention. Then, three maps of attention are combined to the A_{patch} attention map comprehensively using the summation of element-wise activated using the σ sigmoid function later.

$$A_{\text{patch}} = \sigma\left(A_{\text{average}} + A_{\text{max}} + a\right) \tag{7}$$

Lastly, the existing representations globally are multiplied, having the maps of patch attention for producing the Global as feature representation of global attention aware.

$$A_{\text{patch}} = \sigma\left(A_{\text{average}} + A_{\text{max}} + a\right) \tag{8}$$

Here, the multiplication of tensor is presented as $\otimes$. The proposed attention of pooling is not considering all the features of the map rather than depending on the most discriminant patch, yet providing various weights to every patch rather than merging all the patches in an equal way that is apart from the traditional average pooling and max pooling. Hence, attention pooling emphasises the feature representation to enlighten noise interference for the critical patches. On the other hand, the connection remains between the patches of key and unwanted patches for eliminating the loss of the relevant features, potentially enhancing the classification performance and lowering the rate of misdiagnosis for particular subjects. More particularly, the pathological locations are identified using the patch attention map that is a reference.

3.4 | Global network layer

Figure 1 shows the global classifier with attention awareness to continue representing the Global as bag-level, considering higher correlations between the patches and generating the final diagnosis. The CL give the supreme higher level extraction of feature abilities on the inter-patch features for DL compared with direct, FCL for exploring the correlation between the features. Then, two layers of the convolutional network are used for learning the feature representation based on attention awareness in front of the global classifier from the pooling to extract more information related to structure between features and patches with channels. There are two CL with 64 and 128 filters, each having a $2 \times 2 \times 2$ similar size and unit stride that follows using the BN (batch normalisation) and ReLU activations (rectified linear unit). Thus, the down-sampling of the feature maps to $F \in R^{64^*1^*1^*1}$ is chosen by the adaptive 3D average pooling. Thus, the representation of the feature is flattened like the consecutive two fully connected layers as the input having 2 and 32 units for creating two scores that are normalised using the softmax function to present the positive and negative probability accordingly. The attention mechanism is done for learning the integral feature representation for the complete structural information of the brain in the scans of MRI depends on the various output of weighted feature from the attention pooling and the classification of output gives the outcome to predict the MCI conversion or the classification of ES.

3.5 | Loss function

The label of image level is concerned with the peculiar guidance utilised in the backpropagation to update the proposed weights of network W since the labels of image level are provided only during the ambiguous patch-level labels. The loss function is to train the model with cross-entropy loss as it is defined as follows:

$$L(W) = -\frac{1}{N}\sum_{n=1}^{N}\log(P(Y_n|X_n; W)) \quad (9)$$

Here, the number of images is represented as N, and the probability of exact prediction for X_n is represented as $P(Y_n|X_n;W)$. The training losses are backpropagated as the end-to-end network to the Patch-Nets and PAM pooling from the global classifier to assist in updating the network parameters having the optimisation algorithm such as Adam. The proposed network learns the map finally as X to Y to reduce the loss function.

3.6 | Model execution

The activation of batch normalisation is used in the proposed system to alleviate the over-fitting problem after CL. Patches are made for weight sharing and to reduce the trained parameters, particularly during the higher requirement of the cohort patches. Image patches extract patch from various anatomical structures that efficiently augment the diversity to train the data.

The proposed method's performance and generalisability are determined using an EEG dataset. More particularly, the samples are divided in the proposed system from the dataset to train and test with samples as 80% to use for training the model. On the other hand, balance samples of 20% are taken for the test dataset. The hyper-parameters are selected, and the models are trained on the training dataset with 5-fold CV. Thus, the model is trained to have hyper-parameters which are optimised to test to perform the test dataset. The proposed system is determined as the independent dataset to check the generalisability and powerfulness of the proposed model.

The $p-$ value map is computed in the training stage to cover the complete image using the set of comparisons on the training test, that is, 4 subsets for every round in 5-fold for initialising the locations of the input patch. Thus, the patches are extracted to feed from the chosen regions in the images for the relevant patch accordingly. Adam optimiser is used to train the suggested D^2PAM for 100 epochs that has $\sim$ 6 h to determine the balance validation. Hyper-parameters such as the number of channels and rate of learning is 0.001, the size of the batch is 10, the size of the patch is 25 × 25 × 25, and the number of patches is 60 to select using the mean performance validation over all the folds. The patches are extracted at a similar location utilised in the training phase from the unseen image for the diagnosis of ES to the trained network in the test stage depending on the pre-processed image that considers $\sim$ 0.25.

4 | EXPERIMENTAL RESULTS

The evaluation of the anticipated method is validated using certain standard classification approaches. The proposed D^2PAM model is evaluated with various existing approaches.

4.1 | Dataset

The significance of the anticipated model is examined using the EEG signals for seizure and healthy signal classification. Here, the dataset is acquired from online resources, that is, Bonn University, which is a public and open source dataset with various groups, that is, A to E. Every group is sensed in various conditions and recorded in diverse conditions of the subjects. Dataset A and B are determined to be healthy and recorded during awake conditions. Then, C and D are monitored during inter-ictal period and E group is known as ictal period. The recorded signals with 23s duration use a 10–30 electrode system with a 173.6 Hz sampling rate. Every group in the dataset is composed of single EEG channel epochs with a 4097 sampling rate.

4.2 | Metrics

The measurements are evaluated, such as precision, accuracy, sensitivity as recall, false alarm rate (FAR), area under the curve (AUC) and f1-score are presented below.

$$\text{Accuracy} = \frac{TP + TN}{TP + TN + FP + FN} \quad (10)$$

$$\text{Recall or sensitivity} = \frac{TP}{TP + FN} \quad (11)$$

$$\text{Precision} = \frac{TP}{TP + FP} \quad (12)$$

$$F1 - \text{score} = 2 * \frac{\text{precision} * \text{recall}}{\text{precision} + \text{recall}} \quad (13)$$

$$FAR = \frac{FP}{FP + TN} \quad (14)$$

Here, the total true pre-seizure as pre-ictal segments of EEG is presented by TP, FN presents the total false no-seizure segments of D^2PAM, and TN presents the total true normal as no-seizure for the segments of D^2PAM, and FP presents the total false pre-ictal segments of D^2PAM. The model's performance is evaluated using the F1 score in the unbalanced data. FAR is utilised frequently for measuring Epilepsy misreporting using the software in the clinical epilepsy diagnosis. Under the ROC curve, the area definition for AUC is presented.

4.3 | Experimental setup

Here, leave-one-out is used to check the model's performance and five samples are chosen, which has no-seizure EEG data and pre-ictal EEG data is testing data and the balanced data is training data. The conventional method like SVM [31], Diffusion Convolutional Neural Network (D-CNN) D-CNN [33], Deep Convolutional Neural Network (DP-CNN) [33], CNN-based voting [32], Partial Interpretable Estimators (PIES) [34], Transformer [35], Long Short Term Memory (LSTM) [36], ED-ANN with LSTM [37] and ED-ANN with transformer [38] are used for comparison, as shown in Table 2. Data pre-processing and various data input are employed for all the methodologies. The data has the hidden representation for every window with size of 1s. The model provides the result from prediction for every window with a size of 1 s. The classifiers like DP-CNN and CNN-voting shows window data representation when the size of the window as 1s. EEG seizure based adversarial learning known as PIES (Patient-Independent Epileptic Seizure) is used for classification where PIES has the fixed input of data length. The researchers report that the experiment's setting is used in the proposed system is to lower the input data length to 1 s. On the other hand, experimental outcomes are compared to replace the domain category discriminator which uses similar CNN encoder. Four CL exist in the encoder, four ReLu regularisation functions, four max-pooling layers, and the dropout layer as 0.5. Lastly, the hidden vector has a dimension of 32. A similar domain discriminator of BiLSTM is used by both models with 64 hidden units and 2 bidirectional LSTM layers. The important discrimination among LSTM and D^2PAM is considered. The label classifier and similar encoder module are there. The proposed system uses a similar structure to the EDANNTransformer for classification purpose. Also, data pre-processing is used by all of the method where 0.0005 is set as the rate of learning α of the D^2PAM model. The D^2PAM model is implemented on the framework of Pytorch and to deploy having the Intel i9 CPU. The model is trained to complete by using the 14 h on average.

4.4 | Experimental outcomes

The proposed D^2PAM system has the performance, and the benchmark model is presented in Table 3 for the 5 test patients on the data. Tables 3-5 present the examination results that the domain-based adversarial model classification method is suggested to obtain better outcomes. The methodology depends on the D^2PAM obtaining better outcomes in terms of F1- score on all the patients in a specific manner. The proposed system performs well than the model of benchmark using the approximate 4.5% concerning the F1 score presented in Tables 4 and 5. It is possible because of the EEG signal nature. The characteristics of Epilepsy for a few people are very obvious for the simple model to perform better due to the signal of EEG, including the characteristics of a non-stationary one. The model of D^2PAM performs well than the model of baseline using the approximation of 9% concerning the F1 score based on Tables 3-5, which provides the concept of using the adversarial learning of domain that lower the interference of every information efficiently. On the other hand, the table values gives the method of PIESD that depends on adversarial learning to perform as same as the common method based on CNN. Tables 3-5 give the comparison of the proposed model with the various existing approaches. The comparison is made among the proposed and the existing SVM, D-CNN, DP-CNN, CNN-based voting, PIES, LSTM, transformer, ED-ANN with LSTM and ED-ANN with transformer.

The proposed D^2PAM model concerning FAR is stable, having less FAR that is essential in the practical applications of clinics. The above tables present the data examination with the proposed model having a bad index of FAR of 3%, which shows better performance. The D^2PAM model is used to compare the performance having the various methods of channel order on the five patients to check the reordering effect of the segment rows of EEG in the pre-processing of data. The default channel order of EEG uses the Random as the sorting of EEG default order based on the ID channel. The D^2PAM has the performance to show from the results of experiments on the data after reordering the channel is 6% best over the average to prove the efficiency of the pre-processing of data.

The accuracy is compared in the proposed system for the data having various lengths since the proposed system utilises the data of variable length to train. The process of varying the model's accuracy using D^2PAM is presented in Figures 2–11, with various lengths of fragment sizes. If the length of the fragment is lower than 5 s, the accuracy rate is increased rapidly with the length of the fragment. The proposed model has the accuracy increased slowly if the size of fragment length is 5–10, like the increases in the length of the fragment. Also, the proposed model has the accuracy unchanged in the basic form if the length of the fragment is greater than 10s when length is higher. The proposed D^2PAM system needs a particular size fragment length for obtaining suitable signals. The proposed D^2PAM model obtains the amount of information that lowers the length of the fragment to increase the wrong prediction for the likelihood. Moreover, the noise is increased in the data for too long fragments, which lowers the accuracy. The optimum recognition for the fragment length shown by the experiments is approximated to 10 s. Physicians need time in the clinic to predict the characteristic signals of Epilepsy is approximate 10 s, that is, consistently having the results from the experiments.

A considerable influence on the accuracy is obtained by using the parameter γ in the experiment. The parameter γ influences 0–0.5 and is explored in the proposed system on the model of D^2PAM for the patient-1EEG data. Figure 2 observes that the model's accuracy increases, increasing γ if γ is lesser than 0.3. The model's accuracy reached the highest value, approximately 95% and increased by γ, and the model's accuracy decreases gradually if γ is 0.3. The domain discriminator contribution for the complete model is less relative, and the system learns the incorrect data easily regarding the patient that turns to the less performance of the model if γ is less. The interference of the domain discriminator is done by having the label classifier learn if γ is higher than 0.3 and the model's accuracy is lowered. The discriminator of the domain is essential for the model of D^2PAM for approximate functioning. The ablation experiment is performed in the proposed system for further research on the domain discriminator influence and the experiment's label classifier, where the discriminator of the domain defines to remove the domain discriminator and add the domain discriminator using discriminator. The Transformer and LSTM are used in to compare the results of the F1-score as the label classifier. Tables 3-6 give the higher impact by the domain discriminator

TABLE 3 Performance evaluation using data on patient 1.

Techniques	Accuracy	Precision	Recall	F1-score	AUC	FAR
SVM	79 ± 0.03	38 ± 0.01	42 ± 0.03	40 ± 0.07	64 ± 0.01	0.13 ± 0.03
D-CNN	83 ± 0.03	50 ± 0.03	90 ± 0.02	65 ± 0.08	91 ± 0.02	0.17 ± 0.03
DP-CNN	88 ± 0.01	61 ± 0.01	76 ± 0.03	68 ± 0.05	92 ± 0.03	0.09 ± 0.03
CNN-based voting	88 ± 0.03	68 ± 0.01	53 ± 0.04	59 ± 0.02	87 ± 0.04	0.14 ± 0.03
PIES	89 ± 0.01	69 ± 0.03	80 ± 0.01	74 ± 0.09	91 ± 0.05	0.08 ± 0.03
LSTM	90 ± 0.01	66 ± 0.02	74 ± 0.03	70 ± 0.02	79 ± 0.01	0.15 ± 0.03
Individual transformer	73 ± 0.01	70 ± 0.01	79 ± 0.04	68 ± 0.01	80 ± 0.02	0.18 ± 0.03
ED-ANN with LSTM	72 ± 0.03	70 ± 0.02	67 ± 0.02	79 ± 0.03	96 ± 0.03	0.03 ± 0.03
ED-ANN with transformer	91 ± 0.10	86 ± 0.02	87 ± 0.08	86 ± 0.04	97 ± 0.04	0.02 ± 0.03
Deep dual-patch attention mechanism (D^2PAM)	95 ± 0.09	90 ± 0.01	92 ± 0.04	90 ± 0.03	98 ± 0.03	0.01 ± 0.03

TABLE 4 Performance evaluation using data on patient 2.

Techniques	Accuracy	Precision	Recall	F1-score	AUC	FAR
SVM	93 ± 0.03	76 ± 0.01	84 ± 0.03	80 ± 0.07	89 ± 0.01	0.05 ± 0.03
D-CNN	87 ± 0.03	56 ± 0.03	96 ± 0.02	71 ± 0.08	96 ± 0.02	0.14 ± 0.03
DP-CNN	96 ± 0.01	83 ± 0.01	92 ± 0.03	87 ± 0.05	90 ± 0.03	0.02 ± 0.03
CNN-based voting	90 ± 0.03	64 ± 0.01	90 ± 0.04	75 ± 0.02	98 ± 0.04	0.10 ± 0.03
PIES	94 ± 0.01	78 ± 0.03	80 ± 0.01	79 ± 0.09	94 ± 0.05	0.05 ± 0.03
LSTM	95 ± 0.01	79 ± 0.02	94 ± 0.03	86 ± 0.02	97 ± 0.01	0.04 ± 0.03
Individual transformer	96 ± 0.01	88 ± 0.01	88 ± 0.04	86 ± 0.01	98 ± 0.02	0.05 ± 0.03
ED-ANN with LSTM	97 ± 0.03	94 ± 0.02	93 ± 0.02	93 ± 0.03	98 ± 0.03	0.011 ± 0.03
ED-ANN with transformer	98 ± 0.10	94 ± 0.02	95 ± 0.08	94 ± 0.04	98 ± 0.04	0.011 ± 0.02
Deep dual-patch attention mechanism (D^2PAM)	99 ± 0.09	95 ± 0.01	96 ± 0.04	96 ± 0.03	99 ± 0.03	0.0117 ± 0.03

TABLE 5 Performance evaluation using data on patient 3.

Techniques	Accuracy	Precision	Recall	F1-score	AUC	FAR
SVM	90 ± 0.03	91 ± 0.01	90 ± 0.03	90 ± 0.07	98 ± 0.01	0.13 ± 0.03
D-CNN	98 ± 0.03	97 ± 0.03	93 ± 0.02	95 ± 0.08	99 ± 0.02	0.04 ± 0.03
DP-CNN	96 ± 0.01	93 ± 0.01	96 ± 0.03	93 ± 0.05	96 ± 0.03	0.01 ± 0.03
CNN-based voting	97 ± 0.03	94 ± 0.01	86 ± 0.04	90 ± 0.02	99 ± 0.04	0.14 ± 0.03
PIES	97 ± 0.01	93 ± 0.03	97 ± 0.01	95 ± 0.09	98 ± 0.05	0.02 ± 0.03
LSTM	98 ± 0.01	93 ± 0.02	98 ± 0.03	95 ± 0.02	98 ± 0.01	0.15 ± 0.03
Individual transformer	98 ± 0.01	92 ± 0.01	99 ± 0.04	95 ± 0.01	99 ± 0.02	0.18 ± 0.03
ED-ANN with LSTM	98 ± 0.03	95 ± 0.02	95 ± 0.02	95 ± 0.03	99 ± 0.03	0.03 ± 0.03
ED-ANN with transformer	98 ± 0.10	97 ± 0.02	95 ± 0.08	97 ± 0.04	99 ± 0.04	0.02 ± 0.03
Deep dual-patch attention mechanism (D^2PAM)	99 ± 0.09	98 ± 0.01	99 ± 0.04	98 ± 0.03	99 ± 0.03	0.01 ± 0.03

from the experiment on the F1-score. More specifically, the D^2PAM model has a more pronounced impact.

Various existing approaches are widely adopted for analysing the neurological disorder which is the reflection of brain variations. Moreover, owing to the local atrophy, some brain regions show structural variations which are extremely correlative with pathological features. However, the primary challenge is to enhance the prediction of discriminative features. To address these issues, the proposed D^2PAM model is adopted for earlier prediction of ES. The proposed model uses

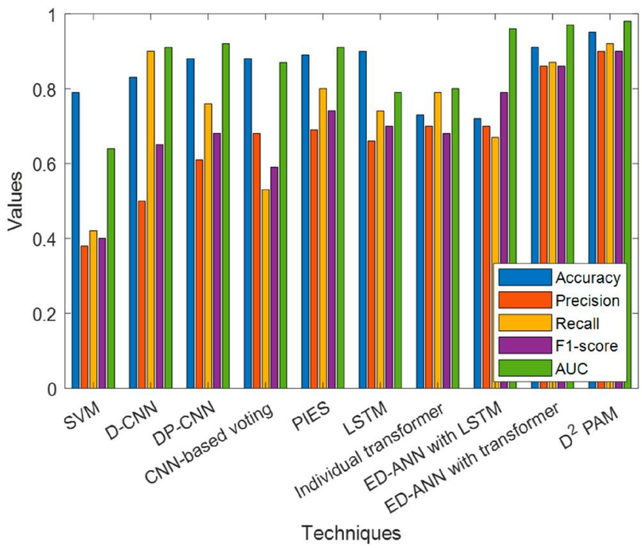

FIGURE 2 Comparison of performance metrics with Patient data 1.

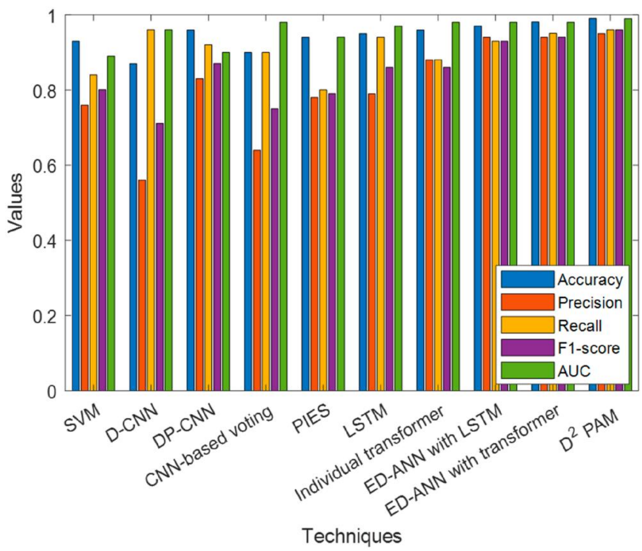

FIGURE 3 Comparison of performance metrics with Patient data 2.

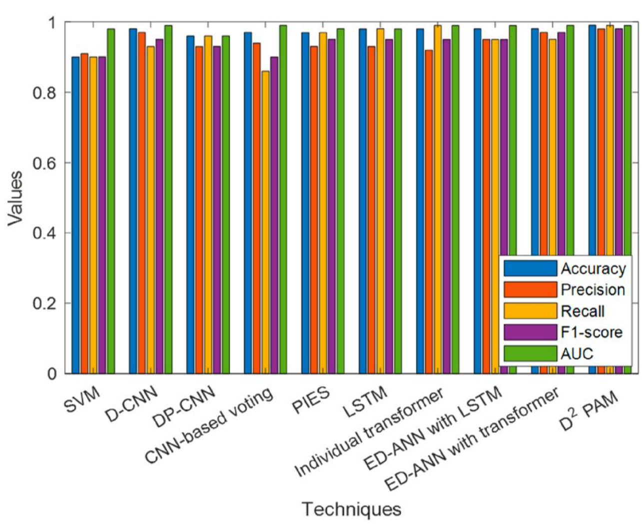

FIGURE 4 Comparison of performance metrics with Patient data 3.

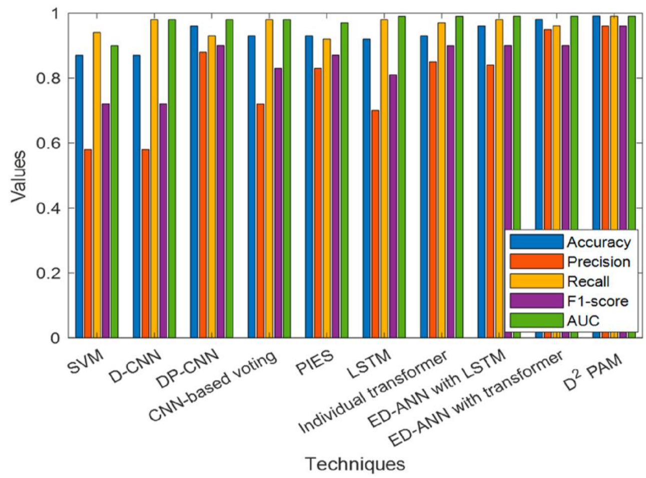

FIGURE 5 Comparison of performance metrics with Patient data 4.

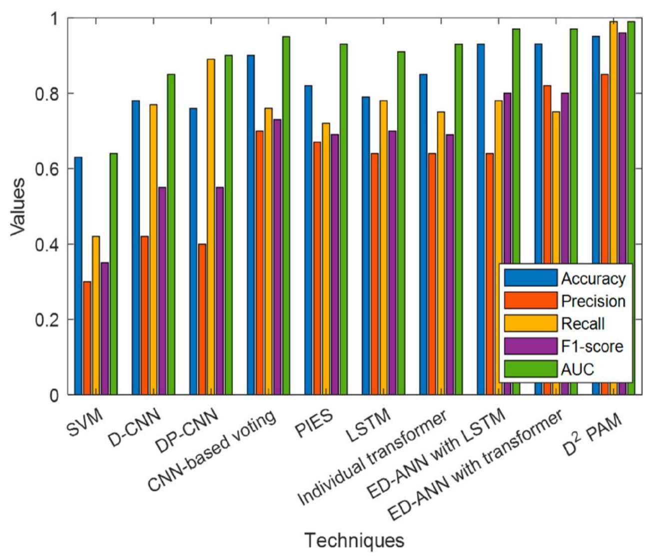

FIGURE 6 Comparison of performance metrics with Patient data 5.

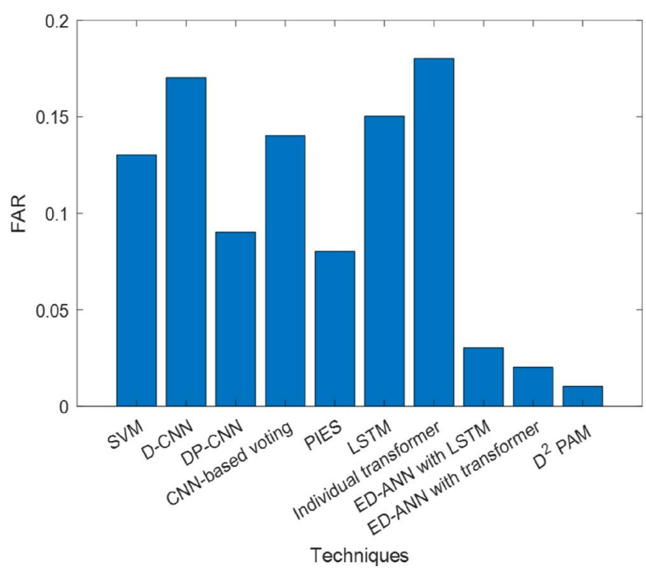

FIGURE 7 False alarm rate with patient 1.

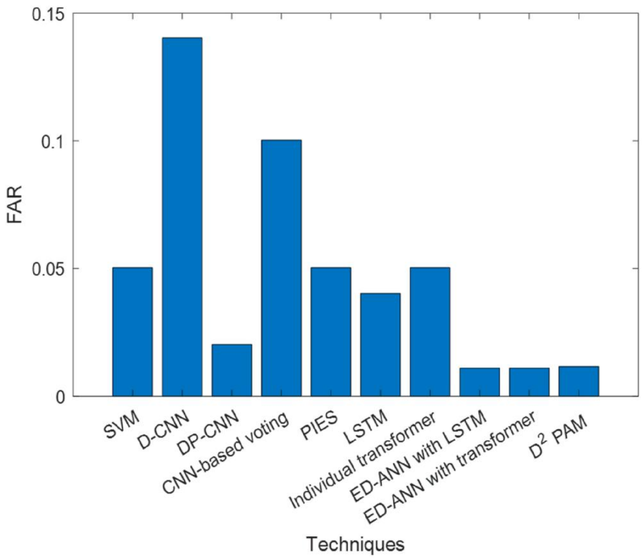

FIGURE 8 False alarm rate with patient 2.

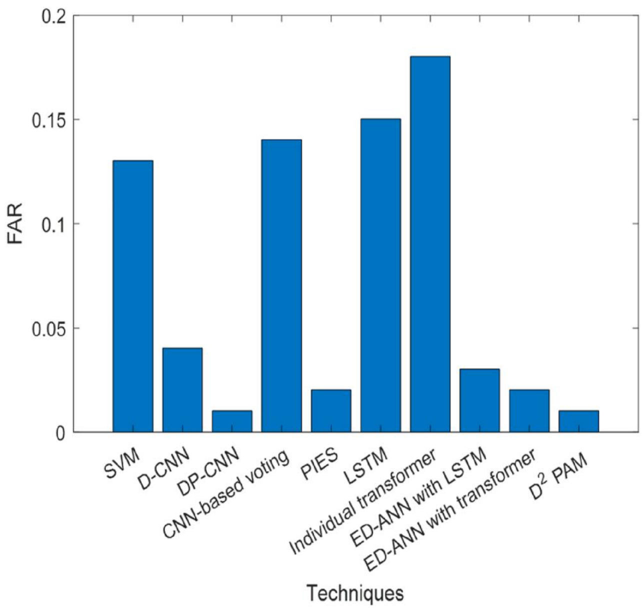

FIGURE 9 False alarm rate with patient 3.

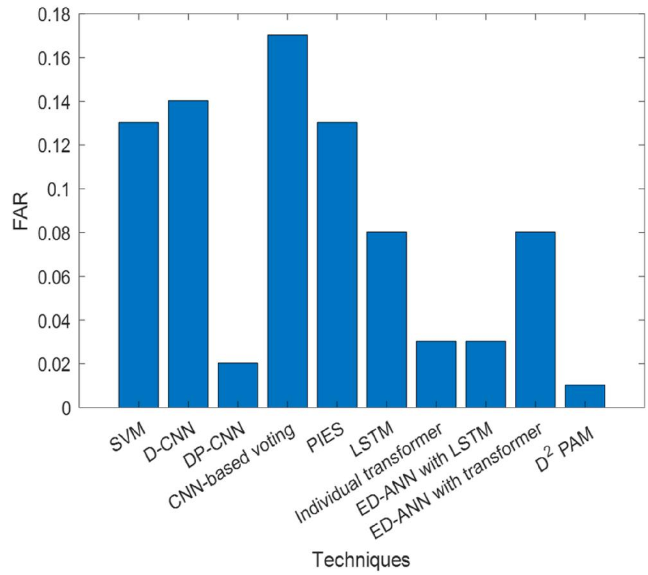

FIGURE 10 False alarm rate with patient 4.

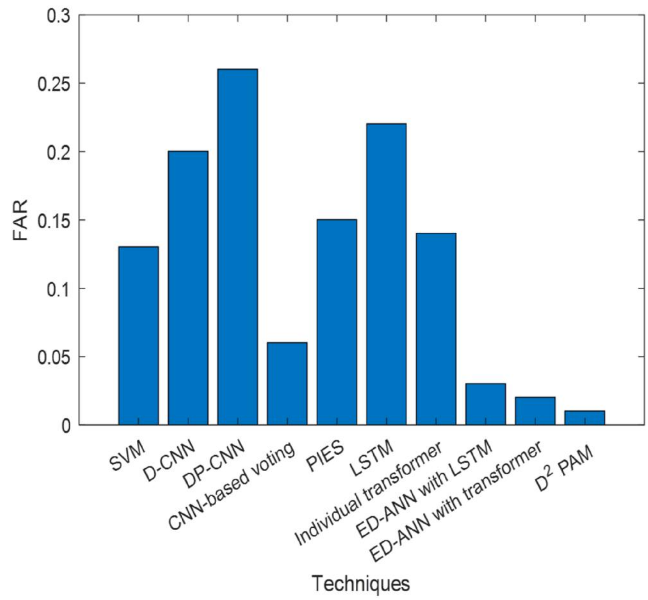

FIGURE 11 False alarm rate with patient 5.

patch network, attention model for analysing the global features for the entire brain information. Based on this, a global classifier model is proposed for ES prediction. In terms of practical implementation, neurophysiologists can find vital patters with the help of the proposed methodology, which leads to the suitable, accurate, and timely treatment of patients.

4.5 | Discussions

The accuracy of the proposed model for sample 1 is 95%, precision is 90%, recall is 92%, F1-score is 90%, AUC is 98% and FAR is 0.01. The accuracy of the proposed model for sample 2 is 99%, precision is 95%, recall is 96%, F1-score is 96%, AUC is 99% and FAR is 0.0117. The accuracy of the proposed model for sample 3 is 99%, precision is 98%, recall is 99%, F1-score is 98%, AUC is 99% and FAR is 0.01. The accuracy of the proposed model for sample 4 is 99%, precision is 96%, recall is 99%, F1-score is 96%, AUC is 99% and FAR is 0.01. The accuracy of the proposed model for sample 5 is 95%, precision is 85%, recall is 99%, F1-score is 96%, AUC is 98% and FAR is 0.01. Based on the analysis with the provided samples, it is proven that the model gives better prediction outcomes than the other approaches.

Figures 2–6 emphasise the comparison of accuracy, precision, recall, F1-score, AUC and FAR results of five patients. In

TABLE 6 Performance evaluation using data on patient 4.

Techniques	Accuracy	Precision	Recall	F1-score	AUC	FAR
SVM	87 ± 0.03	58 ± 0.01	94 ± 0.03	72 ± 0.07	90 ± 0.01	0.13 ± 0.03
D-CNN	87 ± 0.03	58 ± 0.03	98 ± 0.02	72 ± 0.08	98 ± 0.02	0.14 ± 0.03
DP-CNN	96 ± 0.01	88 ± 0.01	93 ± 0.03	90 ± 0.05	98 ± 0.03	0.02 ± 0.03
CNN-based voting	93 ± 0.03	72 ± 0.01	98 ± 0.04	83 ± 0.02	98 ± 0.04	0.17 ± 0.03
PIES	93 ± 0.01	83 ± 0.03	92 ± 0.01	87 ± 0.09	97 ± 0.05	0.13 ± 0.03
LSTM	92 ± 0.01	70 ± 0.02	98 ± 0.03	81 ± 0.02	99 ± 0.01	0.08 ± 0.03
Individual transformer	93 ± 0.01	85 ± 0.01	97 ± 0.04	90 ± 0.01	99 ± 0.02	0.03 ± 0.03
ED-ANN with LSTM	96 ± 0.03	84 ± 0.02	98 ± 0.02	90 ± 0.03	99 ± 0.03	0.03 ± 0.03
ED-ANN with transformer	98 ± 0.10	95 ± 0.02	96 ± 0.08	90 ± 0.04	99 ± 0.04	0.08 ± 0.03
Deep dual-patch attention mechanism (D^2PAM)	99 ± 0.09	96 ± 0.01	99 ± 0.04	96 ± 0.03	99 ± 0.03	0.01 ± 0.03

TABLE 7 Performance evaluation using data on patient 5.

Techniques	Accuracy	Precision	Recall	F1-score	AUC	FAR
SVM	63 ± 0.03	30 ± 0.01	42 ± 0.03	35 ± 0.07	64 ± 0.01	0.13 ± 0.03
D-CNN	78 ± 0.03	42 ± 0.03	77 ± 0.02	55 ± 0.08	85 ± 0.02	0.20 ± 0.03
DP-CNN	76 ± 0.01	40 ± 0.01	89 ± 0.03	55 ± 0.05	90 ± 0.03	0.26 ± 0.03
CNN-based voting	90 ± 0.03	70 ± 0.01	76 ± 0.04	73 ± 0.02	95 ± 0.04	0.06 ± 0.03
PIES	82 ± 0.01	67 ± 0.03	72 ± 0.01	69 ± 0.09	93 ± 0.05	0.15 ± 0.03
LSTM	79 ± 0.01	64 ± 0.02	78 ± 0.03	70 ± 0.02	91 ± 0.01	0.22 ± 0.03
Individual transformer	85 ± 0.01	64 ± 0.01	75 ± 0.04	69 ± 0.01	93 ± 0.02	0.14 ± 0.03
ED-ANN with LSTM	93 ± 0.03	64 ± 0.02	78 ± 0.02	80 ± 0.03	97 ± 0.03	0.03 ± 0.03
ED-ANN with transformer	93 ± 0.10	82 ± 0.02	75 ± 0.08	80 ± 0.04	97 ± 0.04	0.02 ± 0.03
Deep dual-patch attention mechanism (D^2PAM)	95 ± 0.09	85 ± 0.01	99 ± 0.04	96 ± 0.03	9 ± 0.03	0.01 ± 0.03

that, our proposed work D^2PAM achieves higher results than other existing classifiers in all the five patients' data. The numerical comparisons for the five are provided in Tables 3–7. Specifically, the graphical results on FAR are shown from Figures 7–11. In that inference also, the proposed work achieves lesser FAR than the existing models.

Based on the analysis with various observations, it is proven that the model attains competing outcome in ES prediction. When compared to other approaches, the proposed model shows better performance. The reason behind this is that the proposed model deals with the correlation among the features better than the existing approaches. The proposed model tries to extract the essential features which are more difficult in the existing approaches. The proposed model gives better result to project the efficiency of the model for predicting the pathological condition. At last, the proposed model outperforms the existing approaches by demonstrating the finest feature extraction for ES prediction by balancing the contribution of the proposed model.

However, the model attains superior performance in ES prediction; there are still come limitations that influence the generalisation ability of the proposed model. The input patch size is fixed. With the fixed size, feature extraction is completely complex and also the network construction is highly complex. It is essential to merge the patch location generator for prediction of patches for ES prediction. The detection network is optimised as an E2E network model.

5 | CONCLUSION

A Deep dual-patch attention mechanism D^2PAM is suggested in the proposed system for diagnosing computer-aided ES with three important components. They are (i) the discriminative features are extracted from the local patches using the blocks of spatial attention having PatchNets, (ii) the relative contribution of every patch is balanced by using the attention pooling operation, and (iii) the decisions for the ES oriented diagnosis is made by using the attention-aware global classifier depends on the merged representation of feature for the complete structure of the brain. The suggested method of D^2PAM is determined from the dataset in many diagnosis tasks of ES. The proposed system identifies the discriminative pathological locations in the scans of sMRI and obtains the best performance diagnosis over many modern methodologies from the results of experiments. The accuracy of the proposed model for sample 1 is 95%, for sample 2 is 99%, for sample 3 is 99%, for sample 4 is 99%, for sample 5 is 95% respectively.

ACKNOWLEDGEMENT

We would like to acknowledge the Department of Computer Science, College of Computing, Khon Kaen University for its support in conducting this study. Also, the authors are thankful to Chitapong Wechtaisong for its support and fruitful guidance.

CONFLICT OF INTEREST STATEMENT

The authors declare no conflicts of interest.

DATA AVAILABILITY STATEMENT

The data will be available upon request to the corresponding author.

ORCID

Arfat Ahmad Khan https://orcid.org/0000-0003-0918-8874

Rakesh Kumar Madendran https://orcid.org/0000-0002-5059-7269

REFERENCES

1. Freestone, D.R., Karoly, P.J., Cook, M.J.: A forward-looking review of seizure prediction. Curr. Opin. Neurol. 30(2), 167–173 (2017)
2. Kuhlmann, L., et al.: Seizure prediction-ready for a new era. Nat. Rev. Neurol. 14(10), 618–630 (2018). https://doi.org/10.1038/s41582-018-0055-2
3. Hussein, R., et al.: Epileptic seizure detection: a deep learning approach. arXiv preprintarXiv:1803.09848 (2018)
4. Hu, X., et al.: Scalp EEG classification using deep Bi-LSTM network for seizure detection. Comput. Biol. Med. 124, 103919 (2020). https://doi.org/10.1016/j.compbiomed.2020.103919
5. Zhou, M., et al.: Epileptic seizure detection based on EEG signals and CNN. Front. Neuroinform. 12, 95 (2018). https://doi.org/10.3389/fninf.2018.00095
6. Gao, Y., et al.: Deep convolutional neural network-based epileptic electroencephalogram (EEG) signal classification. Front. Neurol. 11, 1–11 (2020). https://doi.org/10.3389/fneur.2020.00375
7. Truong, N.D., et al.: Convolutional neural networks for seizure prediction using intracranial and scalp electroencephalogram. Neural Netw. 105, 104–111 (2018). https://doi.org/10.1016/j.neunet.2018.04.018
8. Ullah, I., et al.: An automated system for epilepsy detection using EEG brain signals based on deep learning approach. Expert Syst. Appl. 107, 61–71 (2018). https://doi.org/10.1016/j.eswa.2018.04.021
9. Acharya, U.R., Hagiwara, Y., Adeli, H.: Automated seizure prediction. Epilepsy Behav. 88, 251–261 (2018). https://doi.org/10.1016/j.yebeh.2018.09.030
10. Malasinghe, L.P., Ramzan, N., Dahal, K.: Remote patient monitoring: a comprehensive study. J. Ambient Intell. Hum. Comput. 10(1), 57–76 (2019). https://doi.org/10.1007/s12652-017-0598-x
11. Singh, K., Singh, S., Malhotra, J.: Spectral features based convolutional neural network for accurate and prompt identification of schizophrenic patients. Proc. Inst. Mech. Eng. Part H J. Eng. Med. 235(2), 167–184 (2021). https://doi.org/10.1177/0954411920966937
12. Singh, K., Malhotra, J.: Stacked autoencoders based deep learning approach for automatic epileptic seizure detection. In: 2018 First International Conference on Secure Cyber Computing and Communication (ICSCCC), pp. 249–254. IEEE (2019)
13. Oh, S.L., et al.: A novel automated autism spectrum disorder detection system. Complex Intell. Syst. 7(5), 2399–2413 (2021). https://doi.org/10.1007/s40747-021-00408-8
14. Ibrahim, F.E., et al.: Deep-learning-based seizure detection and prediction from electroencephalography signals. Int. J. Numer. Methods Biomed. Eng. 38(6), 1–30 (2022). https://doi.org/10.1002/cnm.3573
15. Ouichka, O., Echtioui, A., Hamam, H.: Deep learning models for predicting epileptic seizures using iEEG signals. Electronics 11(4), 605 (2022). https://doi.org/10.3390/electronics11040605
16. Liang, D., et al.: Semisupervised seizure prediction in scalp EEG using consistency regularization. J. Healthc. Eng. 2022, 1–10 (2022). https://doi.org/10.1155/2022/1573076
17. Usman, S.M., Khalid, S., Bashir, S.: A deep learning based ensemble learning method for epileptic seizure prediction. Comput. Biol. Med. 136, 104710 (2021). https://doi.org/10.1016/j.compbiomed.2021.104710
18. Singh, K., Malhotra, J.: Cloud-based ensemble machine learning approach for smart detection of epileptic seizures using higher order spectral analysis. Phys. Eng. Sci. Med. 44(1), 313–324 (2021). https://doi.org/10.1007/s13246-021-00970-y
19. Faust, O., et al.: Deep learning for healthcare applications based on physiological signals: a review. Comput. Methods Prog. Biomed. 161, 1–13 (2018). https://doi.org/10.1016/j.cmpb.2018.04.005
20. Usman, S.M., Usman, M., Fong, S.: Epileptic seizures prediction using machine learning methods. Comput. Math. Methods Med. 2017, 1–10 (2017). https://doi.org/10.1155/2017/9074759
21. Cui, S., et al.: Learning EEG synchronization patterns for epileptic seizure prediction using bag-of-wave features. J. Ambient Intell. Hum. Comput., 1–16 (2018). https://doi.org/10.1007/s12652-018-1000-3
22. Duan, L., et al.: Epileptic seizure prediction based on a convolutional recurrent neural network with multi-timescale. In: Intelligence Science and Big Data Engineering. Big Data and Machine Learning, pp. 139–150. Springer, Berlin (2019)
23. Zhang, S., et al.: A lightweight solution to epileptic seizure prediction based on EEG synchronization measurement. J. Supercomput. 77(4), 3914–3932 (2021). https://doi.org/10.1007/s11227-020-03426-4
24. Usman, S.M., Khalid, S., Bashir, Z.: Epileptic seizure prediction using scalp electroencephalogram signals. Biocybern. Biomed. Eng. 41(1), 211–220 (2021). https://doi.org/10.1016/j.bbe.2021.01.001
25. Assi, E.B., et al.: Towards accurate prediction of epileptic seizures: a review. Biomed. Signal Process Control 34, 144–157 (2017). https://doi.org/10.1016/j.bspc.2017.02.001
26. Upadhyay, R., Padhy, P., Kankar, P.: Eeg artefact removal and noise suppression by discrete orthonormal s-transform denoising. Comput. Electr. Eng. 53, 125–142 (2016). https://doi.org/10.1016/j.compeleceng.2016.05.015
27. Singh, K., Malhotra, J.: IoT and cloud computing based automatic epileptic seizure detection using hos features based random forest classification. J. Ambient Intell. Hum. Comput., 1–16 (2019). https://doi.org/10.1007/s12652-019-01613-7
28. Tsipouras, M.G.: Spectral information of EEG signals concerning epilepsy classification. EURASIP J Adv Signal Process 2019(1), 10 (2019). https://doi.org/10.1186/s13634-019-0606-8
29. Sivasaravanababu, S., et al.: An efficient epileptic seizure detection based on tunable Q-wavelet transform and DCVAE-stacked Bi-LSTM model using electroencephalogram. Eur. Phys. J. Spec. Top. 231(11-12), 2425–2437 (2021). https://doi.org/10.1140/epjs/s11734-021-00380-x
30. Yildirim, Ö.: A novel wavelet sequence based on a deep bidirectional LSTM network model for ECG signal classification. Comput. Biol. Med. 96, 189–202 (2018). https://doi.org/10.1016/j.compbiomed.2018.03.016
31. Rafid Ahmad, S.R., et al.: Prediction of epileptic seizures using support vector machine and regularization. In: 2020 IEEE Region 10 Symposium (TENSYMP), pp. 1217–1220. Dhaka (2020)
32. Hassan, F., Hussain, S.F., Qaisar, S.M.: Epileptic seizure detection using a hybrid 1D CNN-machine learning approach from EEG data. J. Healthc. Eng. 2022, 9579422 (2022). https://doi.org/10.1155/2022/9579422
33. Asjid Tanveer, M., et al.: Convolutional neural networks ensemble model for neonatal seizure detection. J. Neurosci. Methods 358, 109197 (2021). https://doi.org/10.1016/j.jneumeth.2021.109197

34. Wang, T., et al.: Partially interpretable estimators (PIE): black-box-refined interpretable machine learning. arXiv preprint arXiv:2105.02410 (2021)
35. Krishna, G., et al.: EEG based continuous speech recognition using transformers. arXiv:2001.00501. [Online]. http://arxiv.org/abs/2001.00501 (2019). Accessed 21 Oct 2019
36. Alhagry, S., Aly, A., El-Khoribi, R.A.: Emotion recognition based on EEG using LSTM recurrent neural network. Int. J. Adv. Comput. Sci. Appl. 8(10), 355–358 (2017)
37. Bongiorni, L., Balbinot, A.: Evaluation of recurrent neural networks as epileptic seizure predictor. Array 8, 100038 (2020). https://doi.org/10.1016/j.array.2020.100038
38. Yan, J., et al.: Seizure prediction based on transformer using scalp electroencephalogram. Appl. Sci. 12(9), 4158 (2022). https://doi.org/10.3390/app12094158

How to cite this article: Khan, A.A., et al.: D^2PAM: epileptic seizures prediction using adversarial deep dual patch attention mechanism. CAAI Trans. Intell. Technol. 8(3), 755–769 (2023). https://doi.org/10.1049/cit2.12261